Letters in Mathematical Physics (2019) 109:1611–1623
https://doi.org/10.1007/s11005-019-01159-x

# Nodal deficiency, spectral flow, and the Dirichlet-to-Neumann map

**Gregory Berkolaiko[1] · Graham Cox[2] · Jeremy L. Marzuola[3]**

Received: 24 May 2018 / Revised: 21 November 2018 / Accepted: 11 January 2019 /
Published online: 24 January 2019


**Abstract**
It has been recently shown that the nodal deficiency of an eigenfunction is encoded in the spectrum of the Dirichlet-to-Neumann operators for the eigenfunction's positive and negative nodal domains. While originally derived using symplectic methods, this result can also be understood through the spectral flow for a family of boundary conditions imposed on the nodal set, or, equivalently, a family of operators with delta function potentials supported on the nodal set. In this paper, we explicitly describe this flow for a Schrödinger operator with separable potential on a rectangular domain and determine a mechanism by which lower-energy eigenfunctions do or do not contribute to the nodal deficiency.

**Keywords** Nodal domains · Nodal sets · Dirichlet-to-Neumann map · Spectral indices

**Mathematics Subject Classification** 58J50 · 35B05 · 35P05 · 35J10

## 1 Introduction

Let $\Omega \subset \mathbb{R}^d$ be a bounded domain with sufficiently smooth boundary, and denote by $\lambda_1 < \lambda_2 \leq \lambda_3 \leq \cdots$ the eigenvaluesof the Laplacian, with eigenfunctions $\phi_1, \phi_2, \ldots,$

✉ Graham Cox
gcox@mun.ca

Gregory Berkolaiko
berko@math.tamu.edu

Jeremy L. Marzuola
marzuola@email.unc.edu

[1] Department of Mathematics, Texas A&M University, College Station, TX 77843-3368, USA

[2] Department of Mathematics and Statistics, Memorial University of Newfoundland, St. John's, NL A1C 5S7, Canada

[3] Department of Mathematics, University of North Carolina at Chapel Hill, CB 3250 Phillips Hall, Chapel Hill, NC 27599-3250, USA

where we have imposed either Dirichlet or Neumann boundary conditions on $\partial\Omega$. As in Sturm–Liouville theory, one is often interested in quantifying the oscillation of $\phi_k$ in terms of the index $k$.

The *nodal domains* of $\phi_k$ are the connected components of the set $\{\phi_k \neq 0\}$. We denote the total number of nodal domains by $\nu(\phi_k)$. Courant's nodal domain theorem says that $\phi_k$ has at most $k$ nodal domains [7]. In other words, the *nodal deficiency*

$$\delta(\phi_k) := k - \nu(\phi_k) \tag{1}$$

is nonnegative. Beyond this, however, little is known. While it has been shown that the deficiency only vanishes for finitely many $k$ [15], it is generally very difficult to compute or even estimate.

In [5] the first author, Kuchment and Smilansky gave an explicit formula for the nodal deficiency as the Morse index of an energy functional defined on the space of equipartitions of $\Omega$. More recently [9], the second two authors, with Jones, have computed the nodal deficiency in terms of the spectra of Dirichlet-to-Neumann operators using Maslov index tools developed in [8,10]. In particular, for a simple eigenvalue $\lambda_k$ with Lipschitz nodal domains, it was shown that

$$\delta(\phi_k) = \operatorname{Mor}\left(\Lambda_+(\epsilon) + \Lambda_-(\epsilon)\right) \tag{2}$$

for sufficiently small $\epsilon > 0$, where $\Lambda_\pm(\epsilon)$ denote the Dirichlet-to-Neumann maps for the perturbed operator $\Delta + (\lambda_k + \epsilon)$, evaluated on the positive and negative nodal domains $\Omega_\pm = \{\pm\phi_k > 0\}$ and Mor denotes the *Morse index*, or number of negative eigenvalues. For more on the spectrum of Dirichlet-to-Neumann operators, see [2,11, 14] and the recent survey [12].

Similarly, if $\phi_*$ is an eigenfunction for a degenerate eigenvalue $\lambda_*$, the same argument yields

$$\delta(\phi_*) = 1 - \dim\ker(\Delta + \lambda_*) + \operatorname{Mor}\left(\Lambda_+(\epsilon) + \Lambda_-(\epsilon)\right). \tag{3}$$

Note that the Dirichlet-to-Neumann maps depend explicitly on the choice of eigenfunction $\phi_* \in \ker(\Delta + \lambda_*)$. In defining the nodal deficiency of $\phi_*$, we let $k = k_* = \min\{n \in \mathbb{N} : \lambda_n = \lambda_*\}$.

Equations (2) and (3) remain valid for the Schrödinger operator $L = -\Delta + V$ with sufficiently regular potential, for instance $V \in L^\infty(\Omega)$. These formulas were originally obtained from a general spectral decomposition formula, derived using symplectic methods in [9]. In Sect. 2, we give a more direct proof using spectral flow. For a fixed $\phi_*$ we construct a monotone family of self-adjoint operators $\{L_\sigma\}_{\sigma\geq 0}$, starting at $L_0 = L$, such that the nodal deficiency of $\phi_*$ equals the number of eigenvalue curves for $L_\sigma$ that pass through $\lambda_* + \epsilon$ for some $\sigma > 0$; see Fig. 1 for an illustration. This invites a question of potentially great significance: *what properties of the eigenpair* $(\lambda_j, \phi_j)$, $\lambda_j \leq \lambda_*$, *determine whether the corresponding spectral flow curve will cross* $\lambda_* + \epsilon$ *and thus contribute to the nodal deficiency of the eigenfunction* $\phi_*$?

The main result of this paper is a beautifully geometric answer to this question on rectangular domains, illustrated in Fig. 2. Informally speaking, the intersecting curves

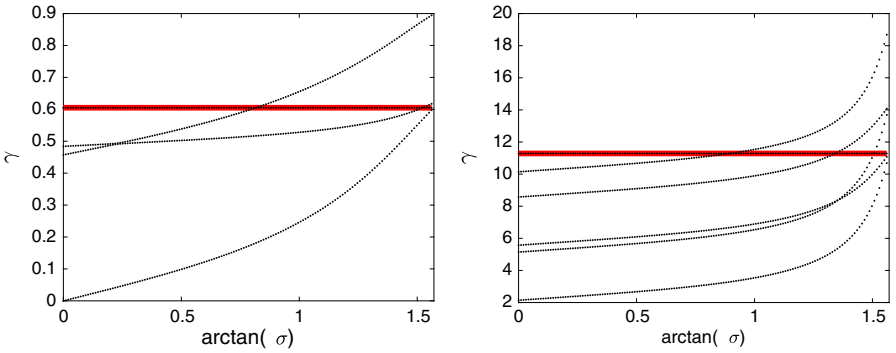


**Fig. 1** Numero-analytic solution of the spectral flow on the tetrahedron quantum graph (left) and on a rectangle (right), as described in Appendix A. In both cases, the number of curves crossing $\lambda_* + \epsilon$ matches the nodal deficiency (2 on the left and 3 on the right)

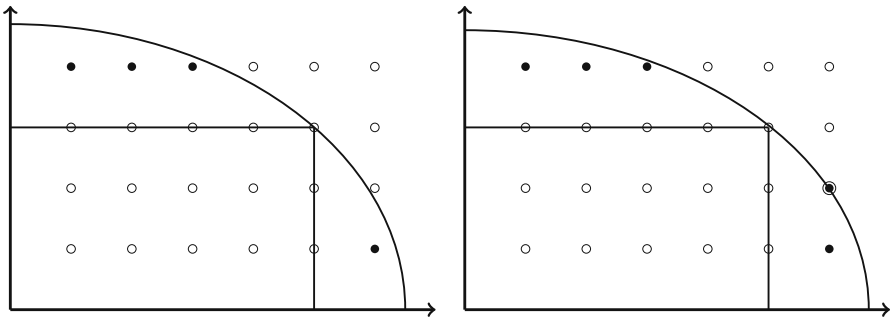


**Fig. 2** The result of Observations 1 and 2. For the simple eigenvalue (**a**), the nodal deficiency is 4, which equals the Morse index of $\Lambda_+ + \Lambda_-$. The degenerate eigenvalue (**b**) also has nodal deficiency 4. The point (6, 2) generates an additional negative eigenvalue of $\Lambda_+ + \Lambda_-$ but does not contribute to the nodal deficiency

arise from the eigenvalues corresponding to the points within the ellipse but outside the rectangle (both regions are specified by $(\lambda_*, \phi_*)$). This geometric interpretation of the nodal deficiency on a rectangle appeared in [3] (see in particular Figure 10). The advantage of our construction is that it describes precisely how these lattice points contribute to the nodal deficiency, through a mechanism (the spectral flow) which is defined on any domain. Before we explain the precise meaning of this statement, we mention that for non-separable problems the situation is likely to be far more complicated due to the presence of avoided crossings; for example, the "intersection" around $\arctan(\sigma) = 0.2$ in Fig. 1(left) is in fact an avoided crossing; see Fig. 3.

Consider the rectangular domain $R_\alpha = [0, \alpha\pi] \times [0, \pi]$ with $\alpha > 0$. We first illustrate our result for the Laplacian, where the computations can be done explicitly. The general statement is formulated and proved in Sect. 4. The spectrum of $-\Delta$ with Dirichlet boundary conditions on $R_\alpha$ is in one-to-one correspondence with the points

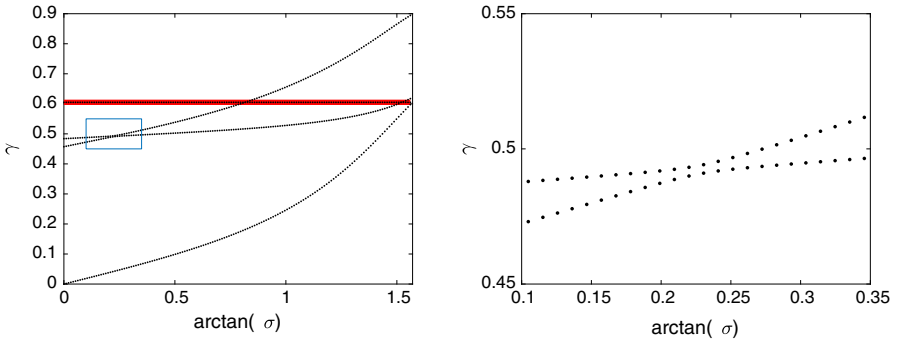


**Fig. 3** Suspected intersection of flow curves for a quantum graph and its zoom

of $\mathbb{N}^2$, namely

$$\sigma(-\Delta) = \left\{ \left(\frac{m}{\alpha}\right)^2 + n^2 \ : \ m, n \in \mathbb{N} \right\}. \tag{4}$$

For a given eigenvalue $\lambda_* = (m_*/\alpha)^2 + n_*^2$, we have $\lambda_* = \lambda_{k_*}$, where

$$k_* = \#\left\{(m,n) : (m/\alpha)^2 + n^2 < \lambda_* \right\} + 1.$$

This counts the lattice points in the region bounded by the quarter ellipse

$$E_{\lambda_*} = \left\{ (x,y) \ : \ x > 0, \ y > 0, \ (x/\alpha)^2 + y^2 < \lambda_* \right\}, \tag{5}$$

plus the point $(m_*, n_*)$, which lies on the ellipse. On the other hand, the corresponding eigenfunction $\sin(m_* x/\alpha)\sin(n_* y)$ has $m_* n_*$ nodal domains, which coincides with the number of lattice points contained in the rectangle

$$R_{\lambda_*} = \{(x,y) \ : \ 0 < x \le m_*, \ 0 < y \le n_*\}. \tag{6}$$

That is, the nodal deficiency equals the number of lattice points under the ellipse but outside the rectangle, as illustrated in Fig. 2.

**Observation 1** *The nodal deficiency of the $(m_*, n_*)$ eigenfunction is equal to the number of lattice points in the region $E_* \setminus R_*$.*

This holds whether or not $\lambda_*$ is simple. When $\lambda_*$ is simple, we conclude from (2) that the Morse index of $\Lambda_+(\epsilon) + \Lambda_-(\epsilon)$ equals the number of lattice points in $E_* \setminus R_*$. On the other hand, when $\lambda_*$ is degenerate, $\Lambda_+(\epsilon) + \Lambda_-(\epsilon)$ has an additional $\dim\ker(\Delta + \lambda_*) - 1$ negative eigenvalues, according to (3). This coincides with the number of lattice points on the ellipse, as shown in Fig. 2b.

**Observation 2** *The Morse index of $\Lambda_+(\epsilon) + \Lambda_-(\epsilon)$ is equal to the number of lattice points in the region $\overline{E_*} \setminus R_*$.*

Using the spectral flow, we prove that this is not just a numerical coincidence—it is precisely the eigenvalues corresponding to points in $\overline{E_*}\backslash R_*$ [via Eq. (4)] that give rise to the spectral flow curves which cross $\lambda_* + \epsilon$ and thus generate negative eigenvalues of $\Lambda_+(\epsilon) + \Lambda_-(\epsilon)$. In Sect. 4, we formalize this statement as Theorem 1 and prove it. The result is valid for any Schrödinger operator with separable potential and hence does not rely on having explicit formulas for the eigenvalues and eigenfunctions, as was the case above.

The spectral flow method can be easily generalized to other settings, such as Schrödinger operators on manifolds and metric graphs. Figure 1(left) shows the results of a numerical computation of eigenvalues of $L_\sigma$ defined on the nodal set of a deficiency 2 eigenfunction of a metric graph (see, for instance, Berkolaiko [4] for an accessible introduction to the subject). Figure 1(right) shows a similar computation for a deficiency 3 eigenfunction of a rectangular domain. In both cases, the number of curves crossing $\lambda_* + \epsilon$ matches the nodal deficiency. As above, the main issue is to determine which eigenpairs $(\lambda_j, \phi_j)$ are responsible for the nodal deficiency.

## 2 The spectral flow

We now describe in more detail the spectral flow mentioned in the introduction, in the process giving a new proof of (2) and (3), and setting the stage for our analysis of the rectangle.

Consider the Schrödinger operator $L = -\Delta + V$ on a bounded, Lipschitz domain $\Omega$, with Dirichlet boundary conditions. Let $\lambda_* \in \text{spec}(L)$, and suppose $\phi_*$ is an eigenfunction for $\lambda_*$, with nodal set $\Gamma = \{x \in \Omega : \phi_*(x) = 0\}$. Throughout this section, we impose the following assumption.

**Hypothesis 1** Each nodal domain of $\phi_*$ has Lipschitz boundary.

For $n = 2$, the hypothesis is always satisfied (see [6, Theorem 2.5]), but its validity appears to be unknown in higher dimensions. In the absence of this assumption one can still define the Dirichlet-to-Neumann maps, following [1], but it is not immediately clear that they will have compact resolvent, and so the spectral flow argument becomes more complicated. We do not pursue this technical issue in the current paper.

We define a family of self-adjoint operators $L_\sigma$ via the bilinear forms

$$B_\sigma(u, v) = \int_\Omega [\nabla u \cdot \nabla v + V u v] + \sigma \int_\Gamma u v \tag{7}$$

on $H_0^1(\Omega)$ for any $\sigma \in [0, \infty)$, and let $L_\infty$ denote the operator with Dirichlet boundary conditions on $\partial\Omega \cup \Gamma$. We denote by $\{\gamma_k(\sigma)\}$ the analytic eigenvalue branches for $L_\sigma$. We first describe the relationship between these eigenvalue curves and the spectrum of $\Lambda_+(\epsilon) + \Lambda_-(\epsilon)$.

**Lemma 1** *For $\epsilon$ sufficiently small, the value $-\sigma$ is an eigenvalue of $\Lambda_+(\epsilon) + \Lambda_-(\epsilon)$ if and only if $\lambda_* + \epsilon = \gamma_k(\sigma)$ for some $k \in \mathbb{N}$.*

***Proof*** First suppose $-\sigma$ is an eigenvalue of $\Lambda_+(\epsilon) + \Lambda_-(\epsilon)$, with eigenfunction $f \in H^{1/2}(\Gamma)$. Then, there is a function $u \in H_0^1(\Omega)$ such that $u\big|_\Gamma = f$, with

$$-\Delta u + Vu = (\lambda_* + \epsilon)u \tag{8}$$

in $\Omega\backslash\Gamma$ and

$$\frac{\partial u}{\partial \nu_+} + \frac{\partial u}{\partial \nu_-} + \sigma u = 0 \tag{9}$$

on $\Gamma$. This means $\lambda_* + \epsilon$ is an eigenvalue of $L_\sigma$, and so $\lambda_* + \epsilon = \gamma_k(\sigma)$ for some $k \in \mathbb{N}$.

Conversely, suppose $\lambda_* + \epsilon = \gamma_k(\sigma)$ for some $k$. The corresponding eigenfunction $u$ will by definition satisfy (8) in $\Omega\backslash\Gamma$ and (9) on $\Gamma$, and so $f := u\big|_\Gamma$ satisfies the eigenvalue equation

$$\Lambda_+(\epsilon) f + \Lambda_-(\epsilon) f + \sigma f = 0.$$

To complete the proof, we must show that $f$ is not identically zero on $\Gamma$. If this was the case, $\lambda_* + \epsilon$ would be an eigenvalue of $L_\infty$, which is not possible because $\lambda_*$ is the first eigenvalue of $L_\infty$ and $\epsilon > 0$ can be taken sufficiently small such that $\lambda_* + \epsilon$ lies in the spectral gap. □

Motivated by this result, we make the following definition.

**Definition 1** An eigenvalue curve $\gamma_k(\sigma)$ is said to give rise to a negative eigenvalue of $\Lambda_+(\epsilon) + \Lambda_-(\epsilon)$ if $\gamma_k(\sigma) = \lambda_* + \epsilon$ for some $\sigma > 0$.

Lemma 1 says that $-\sigma$ is a negative eigenvalue of $\Lambda_+(\epsilon) + \Lambda_-(\epsilon)$ if and only if there is an eigenvalue curve $\gamma_k(\sigma)$ that gives rise to it. In other words, the Morse index of $\Lambda_+(\epsilon) + \Lambda_-(\epsilon)$, and hence the nodal deficiency of the eigenfunction $\phi_*$, is completely determined by the curves $\{\gamma_k(\sigma)\}$. Determining whether or not a given curve intersects $\lambda_* + \epsilon$ for some $\sigma > 0$ is simplified by the following monotonicity result, which says that one simply needs to check the endpoints $\gamma_k(0)$ and $\gamma_k(\infty)$.

**Lemma 2** *If $u_k(\sigma)$ is an analytic curve of normalized eigenfunctions for $\gamma_k(\sigma)$, then*

$$\gamma_k'(\sigma) = \int_\Gamma u_k(\sigma)^2. \tag{10}$$

*If $\gamma_k(0) \in \mathrm{spec}(L_\infty)$, then $\gamma_k(\sigma)$ is constant; otherwise, $\gamma_k(\sigma)$ is strictly increasing.*

The existence of an analytic curve of eigenfunctions for $\gamma_k(\sigma)$ is a consequence of the self-adjointness of $L_\sigma$; see [13].

***Proof*** To simplify the notation, we fix a value of $k$ and let $\gamma = \gamma_k(\sigma)$ and $u = u_k(\sigma)$. The eigenvalue equation $L_\sigma u = \gamma u$ is satisfied if and only if

$$B_\sigma(u, v) = \gamma \langle u, v \rangle \tag{11}$$

for all $v \in H_0^1(\Omega)$, where $\langle \cdot, \cdot \rangle$ denotes the $L^2(\Omega)$ inner product. Differentiating (11) with respect to $\sigma$, we find that

$$B'_\sigma(u, v) + B_\sigma(u', v) = \gamma' \langle u, v \rangle + \gamma \langle u', v \rangle. \tag{12}$$

On the other hand, letting $v = u'$ in (11) leads to $B_\sigma(u, u') = \gamma \langle u, u' \rangle$, and so, evaluating (12) at $v = u$, we obtain

$$\gamma' = B'_\sigma(u, u) = \int_\Gamma u^2$$

as desired.

If $\gamma_k(0) \in \operatorname{spec}(L_\infty)$, the associated eigenfunction $u_k(0)$ vanishes on $\Gamma$, so (9) is satisfied for any value of $\sigma$, and hence, $\gamma_k(0) \in \operatorname{spec}(L_\sigma)$. The analyticity of the eigenvalue curves then implies $\gamma_k(0) = \gamma_k(\sigma)$ for all $\sigma$.

If $\gamma_k(\sigma)$ is not strictly increasing, then $\gamma'_k(\sigma_0) = 0$ for some $\sigma_0$. From (10), we infer that the associated eigenfunction vanishes on $\Gamma$, and hence, $\gamma_k(\sigma_0) \in \sigma(L_\infty)$. The argument in the previous paragraph now implies that $\gamma_k(\sigma)$ is constant, with $\gamma_k(0) = \gamma_k(\sigma_0) \in \operatorname{spec}(L_\infty)$. □

Using Lemmas 1 and 2, we can now verify (2) and (3). Indeed, let $\{\lambda_n(\sigma)\}$ denote the ordered eigenvalues of $L_\sigma$, which are non-decreasing. As $\sigma \to \infty$, they converge to the ordered eigenvalues of $L_\infty$, which by definition has Dirichlet boundary conditions on $\partial\Omega \cup \Gamma$ (cf. [2, Proposition 3]). Since $\lambda_*$ is the first Dirichlet eigenvalue on each nodal domain of $\phi_*$, and hence is simple (on each domain), we have that the first eigenvalue of $L_\infty$ is $\lambda_*$, with multiplicity $\nu(\phi_*)$. It follows that

$$\lim_{\sigma \to \infty} \lambda_n(\sigma) = \lambda_*, \quad 1 \le n \le \nu(\phi_*) \tag{13}$$

and

$$\lim_{\sigma \to \infty} \lambda_n(\sigma) > \lambda_*, \quad n > \nu(\phi_*). \tag{14}$$

If $\lambda_*$ is simple, $L_0$ has precisely $k_*$ eigenvalues $\lambda \le \lambda_*$. Since the first $\nu(\phi_*)$ of these converge to $\lambda_*$ as $\sigma \to \infty$, the remaining $k_* - \nu(\phi_*)$ will converge to values greater than $\lambda_*$. Choosing $\epsilon > 0$ sufficiently small, we conclude that each of these $k_* - \nu(\phi_*)$ eigenvalue curves passes through $\lambda_* + \epsilon$ for some finite $\sigma > 0$, in the process giving rise to a negative eigenvalue of $\Lambda_+(\epsilon) + \Lambda_-(\epsilon)$. This verifies (2). Similarly, if $\lambda_*$ is

degenerate, and we define $k_* = \min\{n \in \mathbb{N} : \lambda_n = \lambda_*\}$, then $L_0$ will have precisely $k_* - 1 + \dim\ker(\Delta + \lambda_*)$ eigenvalues $\lambda \le \lambda_*$, and so $k_* - 1 + \dim\ker(\Delta + \lambda_*) - \nu(\phi_*)$ of them will pass through $\lambda_* + \epsilon$ as $\sigma$ increases from 0 to $\infty$. This verifies (3).

## 3 The one-dimensional case

We now refine the general results of Sect. 2 in the one-dimensional case. Let $\{Z_i\}_{i=1}^m$ be a partition of the interval $[0, \ell]$, so that

$$0 < Z_1 < \cdots < Z_m < \ell.$$

For this partition, and some constant $\sigma \in \mathbb{R}$, we define a self-adjoint operator $L_\sigma$ by

$$L_\sigma = -\frac{\mathrm{d}^2}{\mathrm{d}x^2} + q(x)$$

together with the boundary conditions

$$u(0) = u(\ell) = 0 \tag{15}$$

$$u(Z_i-) = u(Z_i+) \tag{16}$$

$$u'(Z_i+) - u'(Z_i-) = \sigma u(Z_i) \quad \text{for all } 1 \le i \le m. \tag{17}$$

Let $\{\lambda_n(\sigma)\}$ denote the ordered eigenvalues of $L_\sigma$. As $\sigma \to \infty$, these converge to the ordered eigenvalues of $L_\infty$, which has Dirichlet conditions imposed at each $Z_i$. Moreover, if $\{Z_i\}$ is the nodal partition of some Dirichlet eigenfunction $\phi_* = \phi_{k_*}$, the spectrum of $L_\infty$ consists of $\lambda_* = \lambda_{k_*}(0)$, with multiplicity $\nu(\phi_*)$, and other eigenvalues strictly greater than $\lambda_*$.

We also know from Lemma 2 that $\lambda_{k_*}(\sigma)$ is constant. Since each $\lambda_n(\sigma)$ is simple and non-decreasing, this implies

$$\lim_{\sigma\to\infty} \lambda_n(\sigma) = \lambda_*, \quad 1 \le n \le k_* \tag{18}$$

and

$$\lim_{\sigma\to\infty} \lambda_n(\sigma) > \lambda_*, \quad n > k_*. \tag{19}$$

This behavior is illustrated in Fig. 4.

Comparing (18) and (19) to (13) and (14), it follows that $\nu(\phi_*) = k_*$, and so we obtain Sturm's theorem as a consequence of the monotonicity and simplicity of the eigenvalues of $L_\sigma$ in the one-dimensional case.

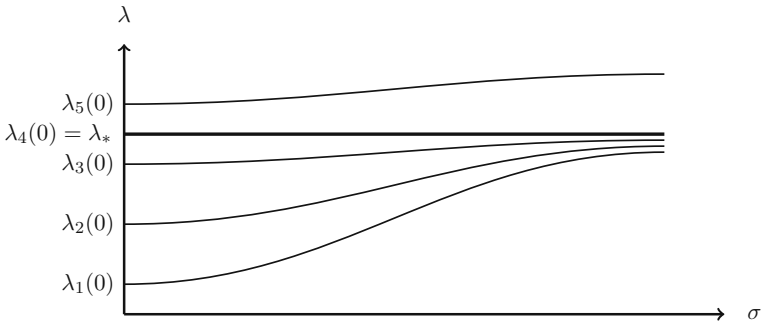


**Fig. 4** The behavior of the first four eigenvalues of $L_\sigma$ in one dimension, with $k_* = 4$. The fourth eigenvalue, $\lambda_4(\sigma) = \lambda_*$, is constant, whereas the first three strictly increase to $\lambda_*$, and the fifth converges to some number strictly greater than $\lambda_*$, as claimed in (18) and (19)

## 4 The rectangle

We now return to the rectangle $[0, \alpha\pi] \times [0, \pi]$, considering a Schrödinger operator

$$L = -\Delta + q(x) + r(y)$$

with separable potential, where $q \in L^\infty(0, \alpha\pi)$ and $r \in L^\infty(0, \pi)$. Let $\{\lambda_m^x\}$ and $\{\lambda_n^y\}$ denote the Dirichlet eigenvalues for $-(\mathrm{d}/\mathrm{d}x)^2 + q(x)$ and $-(\mathrm{d}/\mathrm{d}y)^2 + r(y)$, respectively. The Dirichlet spectrum of $L$ is then given by

$$\mathrm{spec}(L) = \left\{\lambda_m^x + \lambda_n^y : m, n \in \mathbb{N}\right\}.$$

For convenience, we let $\lambda_{mn} = \lambda_m^x + \lambda_n^y$. Now suppose $\lambda_* = \lambda_{m_* n_*} \in \mathrm{spec}(L)$, and let $\Gamma$ denote the nodal set of the corresponding eigenfunction. As above, we define the family $\{L_\sigma\}$ of self-adjoint operators, with analytic eigenvalue curves $\{\gamma_k(\sigma)\}$. Note that $\{\gamma_k(0)\}$ are the eigenvalues of $L$, so for any $(m, n)$ there exists a $k = k(m, n)$ with $\gamma_k(0) = \lambda_{mn}$.

**Definition 2** A lattice point $(m, n)$ is said to give rise to a negative eigenvalue of $\Lambda_+(\epsilon) + \Lambda_-(\epsilon)$ if the curve $\gamma_k(\sigma)$ does, where $k = k(m, n)$ as above.

Our main result, generalizing the picture in Fig. 2, is the following.

**Theorem 1** *The point $(m, n)$ gives rise to a negative eigenvalue of $\Lambda_+(\epsilon) + \Lambda_-(\epsilon)$ if and only if $\lambda_{mn} \le \lambda_*$ and either $m > m_*$ or $n > n_*$.*

That is, the eigenvalue curve $\gamma_k(\sigma)$, with initial value $\gamma_k(0) = \lambda_{mn}$, crosses $\lambda_* + \epsilon$ for some finite, positive value of $\sigma$ if and only if $m$ and $n$ satisfy the given conditions. In the case $V \equiv 0$, these conditions reduce to $(m, n) \in \overline{E_*} \backslash R_*$, as promised in the Introduction.

***Proof*** Let $k = k(m, n)$, so that $\gamma_k(0) = \lambda_{mn} = \lambda_m^x + \lambda_n^y$.

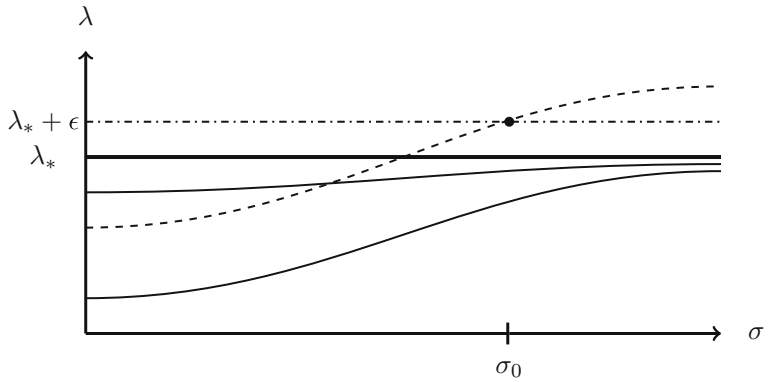


**Fig. 5** The behavior of $\gamma_k(\sigma)$ as $\sigma \to \infty$. The dashed curve has $\gamma_k(0) = \lambda_{mn} < \lambda_*$ and $\gamma_k(\infty) > \lambda_*$, and hence generates a negative eigenvalue $-\sigma_0$ for $\Lambda_+(\epsilon) + \Lambda_-(\epsilon)$. The other two eigenvalue curves correspond to $(m, n) \leq (m_*, n_*)$ and hence stay below $\lambda_*$ for all finite values of $\sigma$

Given $\lambda_* = \lambda^x_{m_*} + \lambda^y_{n_*}$ as above, let $u^x_{m_*}$ and $u^y_{n_*}$ denote the eigenfunctions for $\lambda^x_{m_*}$ and $\lambda^y_{n_*}$, with nodal sets $\{Z^x_k\} \subset (0, \alpha\pi)$ and $\{Z^y_k\} \subset (0, \pi)$, respectively. With respect to these nodal partitions, we define operators $L^x_\sigma$ and $L^y_\sigma$, as in Sect. 3, for $\sigma \in \mathbb{R}$. Denoting the eigenvalues by $\{\lambda^x_m(\sigma)\}$ and $\{\lambda^y_n(\sigma)\}$, we have $\gamma_k(0) = \lambda^x_m(0) + \lambda^y_n(0)$, hence

$$\gamma_k(\sigma) = \lambda^x_m(\sigma) + \lambda^y_n(\sigma) \tag{20}$$

for all $\sigma$.

Since $\gamma_k(\sigma)$ is non-decreasing, the equation $\gamma_k(\sigma) = \lambda_* + \epsilon$ will be satisfied for some $\sigma > 0$ if and only if $\gamma_k(0) \leq \lambda_*$ and $\gamma_k(\sigma) > \lambda_*$ for sufficiently large $\sigma$. The condition $\gamma_k(0) \leq \lambda_*$ is equivalent to $\lambda_{mn} \leq \lambda_*$. On the other hand, it follows from (18) and (19) that

$$\lim_{\sigma\to\infty} \lambda^x_m(\sigma) > \lambda^x_{m_*}$$

if and only if $m > m_*$, and similarly for the limit of $\lambda^y_n(\sigma)$, hence

$$\lim_{\sigma\to\infty} \gamma_k(\sigma) > \lambda^x_{m_*} + \lambda^x_{n_*} = \lambda_*$$

holds if and only if either $m > m_*$ or $n > n_*$ (see Fig. 5 for an example). □

**Acknowledgements** The authors would like to thank Ram Band for interesting discussions and helpful suggestions regarding the manuscript. G.B. acknowledges partial support from the NSF under Grant DMS-1410657. G.C. acknowledges the support of NSERC Grant RGPIN-2017-04259. J.L.M. was supported in part by NSF Applied Math Grant DMS-1312874 and NSF CAREER Grant DMS-1352353.

## Appendix A. Example for a Rectangle

Let us consider first the one-dimensional eigenvalue problem for the case $q(x) = 0$ from Sect. 3. Namely, we wish to compute the eigenvalues $\{\lambda_n(\sigma)\}$ for $\sigma \geq 0$.

### A.1. $\{Z_k\} = \{\frac{1}{2}\ell\}$

The second Dirichlet eigenfunction for the Laplacian the interval $[0, \ell]$ has a zero at $\ell/2$. Using this nodal point to define the boundary conditions in $\sigma$, as in Sect. 3, we look for the eigenvalues $\lambda_n(\sigma)$. We will use the notation $\lambda_n(\sigma; 2)$ to denote the $n$th eigenvalue that arises from the spectral flow in $\sigma$ set at the nodal point of the second Dirichlet eigenfunction. Symmetry considerations guarantee that the corresponding lowest eigenfunction, $u_1(x) = u_1(x, \sigma; 2)$, is symmetric with respect to $\ell/2$. The eigenvalues $\lambda_n(\sigma; 2)$ in this case can be found by taking $u_1(x) = \sin(\kappa x)$ on $[0, \ell/2]$ for $\kappa^2 = \lambda_n$. Condition (17) gives

$$-2u_1'\left(\frac{\ell}{2}\right) = \sigma u_1\left(\frac{\ell}{2}\right),$$

and hence

$$\sigma = -2\kappa \cot\left(\kappa\frac{\ell}{2}\right). \tag{21}$$

Thus, $\lambda_1(\sigma; 2) = \kappa^2$ is given as the implicit solution to (21) for finding the lowest eigenvalue.

### A.2. $\{Z_k\} = \{\frac{1}{3}\ell, \frac{2}{3}\ell\}$

Now, let us consider the next excited state, or the case of the nodal set given by 2 zeros equidistributed throughout the interval. As before, the lowest eigenfunction of $L_\sigma$, denoted $u_1(x) = u_1(x, \sigma; 3)$, is symmetric with respect to $\ell/2$ and we can write

$$u_1(x) = \begin{cases} a\sin(\kappa x), & x \in [0, \ell/3] \\ b\cos(\kappa(\ell/2 - x)) & x \in [\ell/3, \ell/2] \end{cases}$$

Hence, conditions (16) and (17) at $\ell/3$ imply

$$a\sin\left(\frac{\kappa\ell}{3}\right) = b\cos\left(\frac{\kappa\ell}{6}\right) = c,$$
$$-\left(a\kappa\cos\left(\frac{\kappa\ell}{3}\right) - b\kappa\sin\left(\frac{\kappa\ell}{6}\right)\right) = \sigma c,$$

for $c = u_1(\ell/3)$. Solving out for $c$, we arrive at

$$\sigma = \kappa\left(\tan\left(\frac{\kappa\ell}{6}\right) - \cot\left(\frac{\kappa\ell}{3}\right)\right),$$

which can be solved implicitly for $\lambda_1(\sigma; 3) = \kappa^2$.

A similar approach applies to find the second eigenfunction $u_2(x) = u_2(x, \sigma; 3)$, which is anti-symmetric with respect to $\ell/2$. Following the same logic, we arrive at

$$\sigma = -\kappa \left( \cot\left(\frac{\kappa\ell}{3}\right) + \cot\left(\frac{\kappa\ell}{6}\right)\right),$$

which can be solved implicitly for $\lambda_2(\sigma; 3) = \kappa^2$.

### A.3. An example with nodal deficiency 3 on the rectangle

Let us now consider a rectangle of the form $[0, \pi] \times [0, \alpha\pi]$ with $\alpha < 1$ but such that $1 - \alpha \ll 1$. We observe in this case that for the Laplacian with Dirichlet boundary conditions,

$$1^2 + \left(\frac{1}{\alpha}\right)^2 = \lambda_{1,1} < \lambda_{2,1} < \lambda_{1,2} < \lambda_{2,2} < \lambda_{3,1} < \lambda_{1,3} = 1^2 + \left(\frac{3}{\alpha}\right)^2.$$

Therefore, the sixth eigenvalue $\lambda_6 = \lambda_{1,3}$ has 3 nodal domains and therefore nodal deficiency 3, see Fig. 6.

Setting $\lambda_* = \lambda_6 = \lambda_{1,3}$, we obtain the spectral flow

$$\begin{aligned}
\gamma_6(\sigma) &= \lambda_*, \\
\gamma_5(\sigma) &= 3^2 + \lambda_1^y(\sigma; 3), \\
\gamma_4(\sigma) &= 2^2 + \lambda_2^y(\sigma; 3), \\
\gamma_3(\sigma) &= 1^2 + \lambda_2^y(\sigma; 3), \\
\gamma_2(\sigma) &= 2^2 + \lambda_1^y(\sigma; 3), \\
\gamma_1(\sigma) &= 1^2 + \lambda_1^y(\sigma; 3),
\end{aligned}$$

which was the flow depicted in Fig. 1(right). The above equations can be analyzed to show that $\gamma_2$, $\gamma_4$, $\gamma_5$ all cross $\gamma_6$ as $\sigma \to \infty$, whereas $\gamma_1$ and $\gamma_3$ do not.

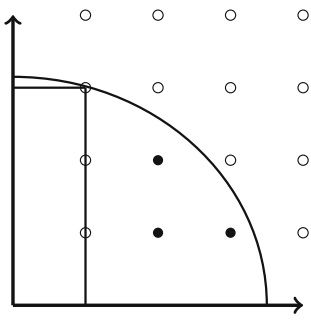

**Fig. 6** The nodal deficiency count for the rectangle example in Appendix A

## References


1. Arendt, W., ter Elst, A.F.M.: The Dirichlet-to-Neumann operator on rough domains. J. Differ. Equ. **251**(8), 2100–2124 (2011)
2. Arendt, W., Mazzeo, R.: Friedlander's eigenvalue inequalities and the Dirichlet-to-Neumann semigroup. Commun. Pure Appl. Anal. **11**(6), 2201–2212 (2012)
3. Band, R., Bersudsky, M., Fajman, D.: Courant-sharp eigenvalues of Neumann 2-rep-tiles. Lett. Math. Phys. **107**(5), 821–859 (2017)
4. Berkolaiko, G.: An elementary introduction to quantum graphs. Geom. Comput. Spectr. Theory **700**, 41 (2017)
5. Berkolaiko, G., Kuchment, P., Smilansky, U.: Critical partitions and nodal deficiency of billiard eigenfunctions. Geom. Funct. Anal. **22**(6), 1517–1540 (2012)
6. Cheng, S.Y.: Eigenfunctions and nodal sets. Comment. Math. Helv. **51**(1), 43–55 (1976)
7. Courant, R., Hilbert, D.: Methods of Mathematical Physics, vol. 1. Interscience Publishers Inc, New York (1953)
8. Cox, G., Jones, C.K.R.T., Marzuola, J.L.: A Morse index theorem for elliptic operators on bounded domains. Commun. Partial Differ. Equ. **40**(8), 1467–1497 (2015)
9. Cox, G., Jones, C.K.R.T., Marzuola, J.L.: Manifold decompositions and indices of Schrödinger operators. Indiana Univ. Math. J. **66**, 1573–1602 (2017)
10. Deng, J., Jones, C.: Multi-dimensional Morse index theorems and a symplectic view of elliptic boundary value problems. Trans. Am. Math. Soc. **363**(3), 1487–1508 (2011)
11. Friedlander, L.: Some inequalities between Dirichlet and Neumann eigenvalues. Arch. Ration. Mech. Anal. **116**(2), 153–160 (1991)
12. Girouard, A., Polterovich, I.: Spectral geometry of the Steklov problem. J. Spectr. Theory **7**(2), 321–359 (2017)
13. Kato, T.: Perturbation Theory for Linear Operators. Grundlehren der Mathematischen Wissenschaften, Band 132, 2nd edn. Springer, Berlin (1976)
14. Mazzeo, R.: Remarks on a paper of Friedlander concerning inequalities between Neumann and Dirichlet eigenvalues. Int. Math. Res. Not. **4**, 41–48 (1991)
15. Pleijel, Å.: Remarks on Courant's nodal line theorem. Commun. Pure Appl. Math. **9**, 543–550 (1956)